International Journal of Automation and Computing
www.ijac.net

18(5), October 2021, 787-801
DOI: 10.1007/s11633-020-1254-z

Robust Observer-based Control of Nonlinear Multi-omnidirectional Wheeled Robot Systems via High Order Sliding-mode Consensus Protocol

M. R. Rahimi Khoygani[1,2] R. Ghasemi[1] P. Ghayoomi[1]

[1] Department of Electrical Engineering, University of Qom, Qom 3716146611, Iran

[2] Department of Control Engineering, Islamic Azad University, Tehran 1477893855, Iran

Abstract: This paper presents a novel observer-based controller for a class of nonlinear multi-agent robot models using the high order sliding mode consensus protocol. In many applications, demand for autonomous vehicles is growing; omnidirectional wheeled robots are suggested to meet this demand. They are flexible, fast, and autonomous, able to find the best direction and can move on an optional path at any time. Multi-agent omnidirectional wheeled robot (MOWR) systems consist of several similar or different robots and there are multiple different interactions between their agents, thus the MOWR systems have complex dynamics. Hence, designing a robust reliable controller for the nonlinear MOWR operations is considered an important obstacles in the science of the control design. A high order sliding mode is selected in this work that is a suitable technique for implementing a robust controller for nonlinear complex dynamics models. Furthermore, the proposed method ensures all signals involved in the multi-agent system (MAS) are uniformly ultimately bounded and the system is robust against the external disturbances and uncertainties. Theoretical analysis of candidate Lyapunov functions has been presented to depict the stability of the overall MAS, the convergence of observer and tracking error to zero, and the reduction of the chattering phenomena. In order to illustrate the promising performance of the methodology, the observer is applied to two nonlinear dynamic omnidirectional wheeled robots. The results display the meritorious performance of the scheme.

Keywords: Multi-agent system (MAS), nonlinear controller, nonlinear observer, high-order sliding mode, consensus protocol, omnidirectional robots.

Citation: M. R. Rahimi Khoygani, R. Ghasemi, P. Ghayoomi. Robust observer-based control of nonlinear multi-omnidirectional wheeled robot systems via high order sliding-mode consensus protocol. *International Journal of Automation and Computing*, vol.18, no.5, pp.787–801, 2021. http://doi.org/10.1007/s11633-020-1254-z

1 Introduction

Nowadays, the evolution of robotics is moving towards the widespread usages of mobile robots (MR) in novel arenas[1,2], like transporting products, force feedback operations, human service, service robotics, and space, etc.[3,4] The MR is commonly used in industrial and commercial applications, e.g., warehouses, industrial, inspection and repair of power transmission lines (smart grids)[5], security, the inspection of agricultural crops on farms[6], helping people in natural disasters[7], military settings[8], the smart interface for interaction with customers[9], hospitals to move materials and also helping people with mobility impairments[10], entertainment, domestic robots, and consumer products such as vacuuming or gardening. The MR can be described as a subset of robotics and information engineering. They are not fixed in a certain place and can freely move in their surroundings, and some of them are autonomous which means they can be navigating a new environment without the need for physical or electromechanical guidance machines. In order to expand the efficiency of transporting products, the MRs and conveyance carriers are applied in hospitals, warehouses, and factories. Moreover, in a relatively controlled space, they use guidance devices that permit them to move on a preset navigation path. On the other hand, industrial robots are usually moving less. In the next 35 years, the population of people who are 60-year-old or above will increase from 12% to 21%, according to reports from some institutions such as the World Health Organization[11] and United Nations[12]. Therefore, the development of the MR can be used as a modern tool to raise the quality of human life for people with mobility impairments and elderly people. Hence, the combination of fixed domotic systems[13] and the MRs[14] can be contributed to supervise or develop some domestic tasks or applied at home within an unstructured environment.

Research Article
Manuscript received March 5, 2020; accepted September 8, 2020; published online February 2, 2021
Recommended by Associate Editor Jin-Hua She
Colored figures are available in the online version at https://link.springer.com/journal/11633

Research on mobile robots is interesting for scientists. Accordingly, there are one or more laboratories focused on MR research in almost every major technical university. The conventional MRs and vehicles are usually moved forward and backward, and steering is applied to move in various directions. On the other hand, these robots must use turnabouts and switchbacks to move in different directions, but environments with many obstacles and narrow passages disrupt efficient motion. Therefore, an omnidirectional wheeled robot is able to move in the diagonal directions and crosswise directly; furthermore, the direction and steering are needed to move front and back. In order to obtain that demand, different mechanisms for the omnidirectional wheeled robot movement are presented and studied[15,16]. In small spaces, the omnidirectional wheeled robots are very capable and follow complex trajectory paths for quick maneuvering. Some of these robots use three wheels, composed of passive rollers with shifted 120 degrees. The inclusion of a small design also minimizes the probability of it getting accidentally caught. The flexibility of the omnidirectional wheeled robot depends on the unique structure of the wheels, e.g., alternate, Mecanum, ball, series, and orthogonal wheels[17], and in models[18,19], the omnidirectional wheeled robots have 3-degree of freedom (DOF). The precise dynamical model to predict the performance of the omnidirectional robots with 3 and 4 wheels are discussed in [20]. In [21], a trajectory tracking controller for the omnidirectional wheeled robot is proposed. The method is used for the problem of regulation and motion. A model with uncertainties in the dynamic system[22], also applies the theory of Lyapunov stability and intelligent control methods, like fuzzy logic control[23], neural networks[24], adaptive and distributed consensus back-stepping control[25]. Input-output linearization by state feedback of the nonlinear synchronous generator in adaptive control is proposed[26].

The sliding mode is a technique to design a robust controller and observer for nonlinear systems operating under uncertainty conditions. It has a simple overall structure, fast response, no sensitivity to the internal parameters, and external disturbances[27], robustness against parameter uncertainty, and existing disturbances[28,29]. In spite of claimed robustness properties, the traditional sliding mode control has a special bug that is the chattering phenomenon. The presence of high-frequency vibrations in the controlled system that these vibrations degrades the system performance and may compromise the overall system stability. For the reduction of the chattering and maintaining the merits of traditional sliding mode, a high order sliding system was presented in [30, 31]. The super twisting algorithm is one of the most applied methods in the high order sliding mode. In [32], a fuzzy sliding-mode consensus controller of networks of uncertain dynamic agents under external disturbances is investigated. Chang et al.[33] present a formation tracking control for the multi-robot systems via an adaptive fuzzy sliding mode formation controller that uses the multi-agent system to accomplish the desired formation. For the determination of the best control strategy[34], single-input multi-output systems are discussed by decoupled and hierarchical sliding mode control. A novel sliding mode control with variable gains is proposed to obtain a reduction of the so-called chattering effect, and also preserves the robust properties of the conventional sliding modes[35]. A realization of consensus under matched uncertainties for reducing the chattering with the second-order sliding mode is investigated in [36]. Designing an observer controller for a nonlinear dynamics system has been evaluated in [37].

A significant field of robotic research is the multi-agent omnidirectional wheeled robot (MOWR) systems. Generally, there are many benefits of such systems, such as adaptability, including greater flexibility, robustness, and applicability to more than a single robot. Using the mathematical model of the multi-agent systems (MASs) and paying extreme attention to the agent dynamics is focused in [38]. The main point of [39] is the investigation of consensus leader-follower multi-agent systems with external disturbances. How to design a distributed control law by using super-twisting is shown in [40], which investigates a new surface of twisted sliding mode for consideration to ensure finite time consensus. To ensure the consensus of MAS is reached in finite time, a novel distributed controller with asymptotic consensus by using directed communication topology is proposed[41]. Evaluating the sliding mode surface by using a sliding mode technique occurs in [8]. According to the prescribed sliding surface, each agent is coupled, and in the limited time, they are able to reach the sliding surface. Compared to the other research, this paper focuses on the nonlinear controller for a class of multi-agent robot models via the high order sliding mode consensus protocol. Designing a robust controller for affine MAS is one of the most innovative methods when comparing with other methods since it uses the sliding mode technique. The stability of the closed-loop system and convergence of the tracking error to zero are both guaranteed in the presence of the noise and disturbances. The consensus protocol, robust, convergence, and stability are the main merits of this controller.

The remainder of this paper is organized as follows. Some mathematical preliminary definitions which include multi-agent systems, graph theory, and Kronecker mathematics are presented in Section 2. Section 3 presents the problem statement of the multi-agent system. Section 4 reveals the observer based controller algorithm for formation tracking of high-order multi-agent systems. Simulation results are presented in Section 5, and conclusions are drawn in Section 6.

2 System formulation, preliminaries, and definitions

This section presents some important preliminary, stability definitions, interaction modeling between the agents and multi-agent systems which rely on graph theory, and Kronecker mathematics[42].

Definition 1. $\dot{x} = f(x,t)$ is considered as a nonlinear dynamical system. $x(t)$ at point t_0 equals x_0 and assumes $x \in \mathbf{R}^n$ that $f(x,t)$ shows a Lipschitz continuous due to x that is uniformly and piecewise continuous during the time t. $f(x,t)$ is a nonlinear dynamical system which makes standard conditions for the uniqueness and existence of solutions.

Definition 2. Consider a point $x^* \in \mathbf{R}^n$ and assume $f(x^*,t) \equiv 0$, so x^* is an equilibrium point of $\dot{x} = f(x,t)$. An equilibrium point is locally stable if all solutions that start near x^* remain near x^* for all time. On the other hand, x^* is locally asymptotically stable, if x^* is locally stable and all solutions starting in the neighborhood of the point x^* tend towards x^* when $t \to \infty$

Definition 3. (Lyapunov theory) Consider $x^* = 0$ that is named the equilibrium point and $\dot{x} = f(x,t)$ that is stable at $t = t_0$, if for all $\varepsilon > 0$ exists a positive parameter such δ, so that:

$$\|x(t_0) - x_e\| < \delta \to \|x(t) - x_e\| < \varepsilon, \quad \forall t \geq t_0.$$

Suppose that the above condition is satisfied for all $x_0 = x(t_0) \in \mathbf{R}^n$, then it can be said the equilibrium point is globally stable. Fig. 1 depicts the geometric inter- pretation of Lyapunov's theorem. At equilibrium points, the stability of Lyapunov is considered to be a very moderate demand.

Definition 4. (Asymptotic stability) An equilibrium point $x^* = 0$ of $\frac{\mathrm{d}}{\mathrm{d}t}x = f(x,t)$ is asymptotically stable at $t = t_0$, when $x^* = 0$ is stable and locally attractive, there is a $\delta(t_0)$ so that:

$$\|x(t_0)\| < \delta \to \lim_{t\to\infty} x(t) = 0.$$

Here, as in definition 1, the asymptotic stability is explained at t_0. For the conditions of uniform asymptotic stability, $x^* = 0$ is uniformly locally attractive and uniformly stable, that mean there is δ independent of t_0,

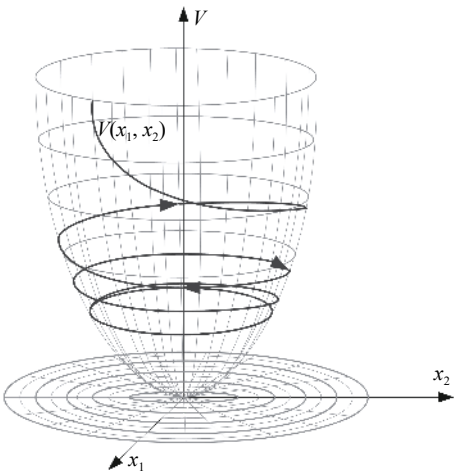

Fig. 1 Geometric interpretation of Lyapunov's theorem

where $\|x(t_0)\| < \delta$ and also it is needed that the convergence in e$\|x(t_0)\| < \delta$ was uniform.

Definition 5. When an derivative of $V(x,t)$ is not definitely locally positive for asymptotic stability of an equilibrium point, Lasalle's theorem can be used. Nevertheless, Lasalle's theorem is used for periodic or autonomous models. Therefore, the autonomous model $\frac{\mathrm{d}}{\mathrm{d}t}x = f(x)$ is as $S(t,\ x_0,\ t_0)$, where it is the solution of $\dot{x} = f(x)$ at time t starting from x_0 at time t_0.

Definition 6. Consider a set S that is a subset of $\mathbf{R}^n$, and also consider a limit set w for the trajectory $S(t, x_0, t_0)$. t_n show a strictly increasing sequence of times, for all $y \in S$, if there exists a t_n,

$$S(t_n, x_0, t_0) \to y \quad \text{when} \quad t_n \to \infty.$$

Definition 7. The set M is a subset of $\mathbf{R}^n$ and is defined as a positively invariant set. Therefore, if for all $\varepsilon > 0$, there exists a positive parameter δ so that $y \in M$ and $t_0 \geq 0$. However, it may be proved that the limitation set w for every path is fixed and closed.

Theorem 1. (Lasalle's theorem) The function V is a subset $\mathbf{R}^n \to \mathbf{R}$ and it is considered as a locally positive definite. On the compact set $\Omega_c = \{x \in \mathbf{R}^n : V(x) \leq c\}$, there is $\dot{V}(x)$ that is locally negative definite ($\dot{V}(x) \leq 0$). Also, $S = x \in \Omega_c$ is defined, so that $(\frac{\mathrm{d}}{\mathrm{d}t})V(x) = 0$ when $t_n \to \infty$ the path tends to the largest invariant set inside S. In other words, the limitation set w is contained inside the largest invariant set in S. In particular, if the set S contains no invariant sets other than $x = 0$, then 0 is asymptotically stable.

2.1 Graph theory and Kronecker mathematics

$\psi = (S, H)$ displays the interaction between the agents and topology where the relation between agents is H and there are a directional arrows in the graph, the set include N agents represented by $S = S_1, \cdots, S_n$. The (S_i, S_j) displays elements of H that is directionally arrowed from S_i to S_j.

Definition 8. It is assumed in the graph that there is not a loop in nodes, the flow of information between two agents is shown by the direction of the arrow. The degree of each node is equal to the arrows entered for each agent and the degree of each agent is equal to the number of arrows out of each agent. If the number of incoming arrows and the number of outgoing arrows for each agent being equal, we can be said that the graph is balanced and otherwise the graph is unbalanced.

Definition 9. a_{ij} is considered as a weight, it is placed between two agents which specifies the amount of information and data exchanged. In this work, all weights are considered as non-zero strictly positive ($a_{ij} > 0$). An undirected graph is meant to satisfy this condition $a_i j = a_j i$ for all nodes, and it turns out that the weights

of the edges (S_i, S_j) and (S_j, S_i) are the same.

Definition 10. The neighbors of each agent are defined as $N_i = j \in S : (i, j) \in \varepsilon,\ j \neq i$ in the MASs. The shortest direction from the agent S_i to the agent S_j is considered as the distance between two agents. On the other hand, the biggest distance between two agents is assumed as the diameter of a graph. δ is defined as the graph tree which all agents except the initial one have one in-degree. The graph tree is also a connected graph, those agents can be expressed as roots because they have one in-degree. The directed tree has taken the form via edges of the graph where this is called the spanning tree in a graph. Most graphs have three matrices as follows:

1) δ is defined as the adjacency matrix which is a square matrix, and the elements of each column of the adjacency matrix a_{ij} specify the communication between node i and node j. Hence, when a_{ij} is 0, it means that there is no communication between the two nodes i and j. Furthermore, if a_{ij} is 1, there is a communication between two nodes.

2) Consider the symbol D as the diagonal matrix, where the principal elements present the degree of that node and other elements equal to 0.

3) The symbol L defines the Laplacian matrix which does a significant task in the analysis of dynamical systems in the graph that can be written as

$$L = D - \delta.$$

2.2 Kronecker mathematics

The symbol $\otimes$ is the Kronecker multiplication that it used in the context of the MASs. This multiplication is defined as follows:

$$\delta \otimes \lambda = [a_{ij}].$$

Consider the matrix $\delta_{m\times n}$ and matrix $B_{P\times q}$, thus $\delta \otimes \lambda$ makes a matrix with dimensions $mp \times nq$:

$$\delta \otimes \lambda = \begin{bmatrix} a_{11}\lambda & a_{12}\lambda & \ldots & a_{1n}\lambda \\ a_{21}\lambda & a_{22}\lambda & \ldots & a_{2n}\lambda \\ \ldots & \ldots & \ldots & \ldots \\ a_{m1}\lambda & a_{n2}\lambda & \ldots & a_{mn}\lambda \end{bmatrix}.$$

Some properties of Kronecker multiplication are proposed as follow:

1-distributive and associative property:

$$\begin{aligned} &\delta \otimes (\lambda + C) = \delta \otimes \lambda + \delta \otimes C \\ &(\delta + \lambda) \otimes C) = \delta \otimes C + \lambda \otimes C \\ &(K\delta) \otimes \lambda = K(\delta \otimes \lambda) = \delta \otimes (K\lambda) \\ &\delta \otimes \lambda = P(\lambda \otimes \delta)Q,\ \ P = Q^{\mathrm{T}}. \end{aligned}$$

In the above equations, all the dimensions of the matrices are the same.

$$(\delta \otimes \lambda)(C \otimes D) = (\delta C) \otimes (\lambda D).$$

2-multiplicative inverse, transpose, conjugate Kronecker multiplication, and absolute value Kronecker multiplication:

$$\begin{aligned} &(\delta \otimes \lambda)^{-1} = \delta^{-1} \otimes \lambda^{-1} \\ &(\delta \otimes \lambda)^{\mathrm{T}} = \delta^{\mathrm{T}} \otimes \lambda^{\mathrm{T}} \\ &(\delta \otimes \lambda)^{*} = \delta^{*} \otimes \lambda^{*} \\ &|\delta \otimes \lambda| = |\delta|^{m}|\lambda|^{n} \end{aligned}$$

where δ and λ are matrix with $n \times n$ and $n \times m$ dimensions.

3 Problem statement

An important goal of MAS is to provide the basics of building complicated systems which includes some agents and mechanisms. The reorganization, the coordinating of the agent behavior in goals, knowledge, and planning to resolve the problems are named as the most important part of the MAS. There is not any overall control system (distributed control) and decentralization of the data for the agent′s problems and lack of sufficient knowledge of each agent. Therefore, agents have to communicate with each other to achieve the objectiveness. Fig. 2 shows the geometric interpretation of an example of MAS. The nonlinear dynamical agent is considered as follows:

$$\begin{aligned} &\dot{\beta}_{i,l} = \beta_{i,l+1} \\ &\dot{\beta}_{i,l+1} = \beta_{i,l+2} \\ &\dot{\beta}_{i,l+2} = \beta_{i,l+3} \\ &\ldots \\ &\dot{\beta}_{i,n_i} = f_i(\beta_i) + g_i(\beta_i)u_i + d_i(t) \\ &l = 1, 2, \cdots, n_i - 1 \end{aligned} \tag{1}$$

where $d(t)$ is the noise and disturbance variable, $f_i(\cdot)$ and $g_i(\cdot)$ are the same for all agents and the satisfaction of the Lipchitz have been achieved in (1), therefore:

$$\dot{\beta}_i = \delta_i\beta_i + \lambda_i[f_i(\beta_i) + g_i(\beta_i)u_i + d_i(t)] \tag{2}$$

where δ_i, λ_i are shown as follows:

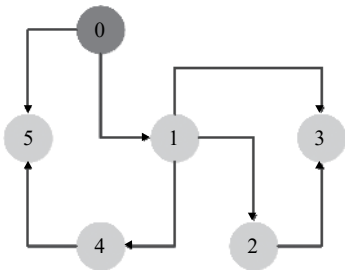

Fig. 2 Geometric interpretation of an example of a multi-agent system

$$\delta_i = \begin{bmatrix} 0 & 1 & 0 & 0 & 0 & ... & 0 \\ 0 & 0 & 1 & 0 & 0 & ... & 0 \\ 0 & 0 & 0 & 1 & 0 & ... & 0 \\ ... & ... & ... & ... & ... & ... & ... \\ 0 & 0 & 0 & 0 & 0 & ... & 1 \\ 0 & 0 & 0 & 0 & 0 & ... & 0 \end{bmatrix}, \lambda_i = \begin{bmatrix} 0 \\ 0 \\ 0 \\ ... \\ 0 \\ 1 \end{bmatrix}. \tag{3}$$

The leader agent can be described as follows:

$$\dot{\beta}_m = \delta_m \beta_m + \lambda_m r_m. \tag{4}$$

The leader agent in (4) leads the other agents to achieve consensus. The agents of the nonlinear MAS are considered as

$$\dot{\beta}_i = (I_N \otimes \delta)\beta_i + \lambda\big[f(\beta) + g(\beta)u + d(t)\big]. \tag{5}$$

The above agents must follow the leader agent and should reach a consensus in a point, therefore, the leader agent dynamic is considered as follows:

$$\dot{\alpha}_m = (I_N \otimes \delta)\alpha_m + \lambda r. \tag{6}$$

Equation (7) shows the overall system as

$$\dot{\alpha} = (I_N \otimes \delta)\alpha + \lambda[f(\beta) + g(\beta)u + d(t)]. \tag{7}$$

The following equation expresses the tracking error H that has an important role in consensus protocol:

$$H = -\Big((L+\lambda) \otimes I_N\Big)(\alpha - \alpha_m). \tag{8}$$

So, by using (8), the tracking error can be written as follows:

$$\dot{H} = -[(L+\lambda) \otimes I_N](\dot{\alpha} - \dot{\alpha}_m). \tag{9}$$

By substituting (6) and (7) into (9), the tracking error can be rewritten as follows:

$$\dot{H} = -[(L+\lambda) \otimes I_N]\Big((I_N \otimes \delta)\alpha + \lambda[f(\beta) + g(\beta)u + d(t)] - (I_N \otimes \delta)\alpha_m - \lambda r\Big). \tag{10}$$

Equation (10) is changed to:

$$\dot{H} = -(I_N \otimes \delta)\Big((L+\lambda) \otimes I_N\Big)(\alpha - \alpha_m) - \Big((L+\lambda) \otimes I_N\Big)\lambda[f(\beta) + g(\beta)u + d(t) - r]. \tag{11}$$

Next with some mathematical manipulations in (11), it can be written as

$$\dot{H} = -\left(\underbrace{I_N \otimes \delta}_{\delta'}\right) H - \left(\underbrace{((L+\lambda) \otimes I_N)}_{L}\lambda[f(\beta) + g(\beta)u + d(t) - r]\right). \tag{12}$$

Then, the tracking error of the overall system is shown as

$$\dot{H} = -\delta' H - L\lambda[f(\beta) + g(\beta)u + d(t) - r]. \tag{13}$$

An observer based on sliding mode technique is considered for the multi-agent model in this work that is given as (14):

$$\dot{\hat{\alpha}}_i = (I_N \otimes \delta)\hat{\alpha} + \lambda[\hat{f}(\beta_i) + g(\beta_i)u + d(t)]. \tag{14}$$

Equation (15) shows the estimation of the tracking error for the multi-agent:

$$\hat{H} = -[(L+\lambda) \otimes I_N](\hat{\alpha_i} - \alpha_m). \tag{15}$$

Hence, the tracking error is defined with (16):

$$\dot{\hat{H}} = -[(L+\lambda) \otimes I_N](\dot{\hat{\alpha}}_i - \dot{\alpha_m}). \tag{16}$$

By substituting (6) and (14) into (16), (17) is obtained as follows:

$$\dot{\hat{H}} = -\left(\underbrace{I_N \otimes \delta}_{\delta'}\right)\hat{H} - \left(\underbrace{((L+\lambda) \otimes I_N)}_{L'}\lambda[\hat{f}(\beta) + \hat{g}(\beta)u + d(t) - r]\right). \tag{17}$$

The estimation of f and g are $\hat{f}(\cdot)$ and $\hat{g}(\cdot)$, also Δf and Δg are defined as $\Delta f = \hat{f} - f$ and $\Delta g = \hat{g} - g$. Therefore, the tracking error of observer for the MAS is as follows:

$$\dot{\hat{H}} = -\delta' \hat{H} - L'\lambda[\Delta f(\beta) + \Delta g(\beta)u + d(t) - r]. \tag{18}$$

Hence, the tracking error dynamic must be minimum which ultimately leads to consensus.

4 Observer based controller for MAS

A high-order sliding mode observer based controller for MAS is presented in this section. The sliding mode observer based controller has two main phases, the reaching and sliding phases. The sliding surface is considered with (19) according to the dynamics (13):

$$Z = \hat{H}. \tag{19}$$

In the reaching phase, the sliding mode can stabilize a time limit for the sliding variable so that $Z = 0$ in the sliding phase. According to the propose sliding surface, the signal of the control is shown as

$$u_{total} = u_{eq} + u_r \tag{20}$$

where u_r and u_{eq} are the reached control input and the equivalent control input. The u_r which is used to remove

certain terms is presented as follows:

$$u_{eq} = \frac{1}{g(\hat{\beta})}\left[f(\hat{\beta}) + d(t) - r + \frac{\delta' H}{L'\lambda}\right] \tag{21}$$

and

$$\begin{cases} g(\hat{\beta}) > g_{\min} \\ \|g(\hat{\beta})\| < g_{\max} \\ \|d(t)\| < d_{\max}. \end{cases} \tag{22}$$

The reach control is used by the high-order algorithm, therefore, u_r is defined as follows:

$$u_r = -k_1 \mathrm{sgn}(z) - k_2 \mathrm{sgn}(\dot{z}), \quad k_1, k_2 > 0. \tag{23}$$

Fig. 3 displays the control scheme based on a leader robot i and follower robot n.

Theorem 2. Consider the multi-agent model (5) and the tracking error of the observer (18). Then the control law (20) causes the state's consensus and will stabilize the overall system and observer.

Proof. In order to prove the stability, a Lyapunov function is considered as

$$L_y = \frac{1}{2}Z^2 \tag{24}$$

to demonstrate the stability of the system must be $\dot{L}_y \leq 0$ and the derivative of the Lyapunov function is $\dot{L}_y = Z\dot{Z}$. Hence, it must be established in the following condition:

$$\dot{L}_y = Z\dot{Z} \leq 0. \tag{25}$$

The inequality $\dot{L}_y = Z\dot{Z} \leq -\eta|Z|$ should be satisfied in order to achieve limited time stability and consensus. So, using (15), (18) and (19) can be rewritten as

$$\dot{L}_y = Z\dot{Z} \leq -\eta|Z| = \hat{H}\big(-\delta'\hat{H} - L'\lambda[f(\beta) + g(\beta)u + d(t) - r]\big) \leq -\eta|Z|. \tag{26}$$

According to control input (20), (26) is rewritten as

$$Z(\lambda u_r) \leq -\eta|Z|. \tag{27}$$

Then, by applying (27), k_1 and k_2 can be derived as $u_r = -k_1\mathrm{sgn}(z) - k_2\mathrm{sgn}(\dot{z})$, where $k_1, k_2 > 0$, then $Z, \dot{Z} \to 0$. Using the variable changing as

$$\zeta_1 = Z \to \dot{\zeta}_1 = \dot{Z} = \zeta_2 \tag{28}$$

$$\zeta_2 = \dot{Z} \to \dot{\zeta}_2 = -k_1\mathrm{sgn}(\zeta_1) - k_2\mathrm{sgn}(\zeta_2). \tag{29}$$

Now, ζ_1, ζ_2 must be 0, because the $Z, \dot{Z} = 0$, therefore the Lyapunov function L_ζ is

$$L_\zeta = \int_0^{\zeta_1} k_1 \mathrm{sgn}(\tau)\mathrm{d}\tau + \frac{1}{2}\zeta_2^2 \tag{30}$$

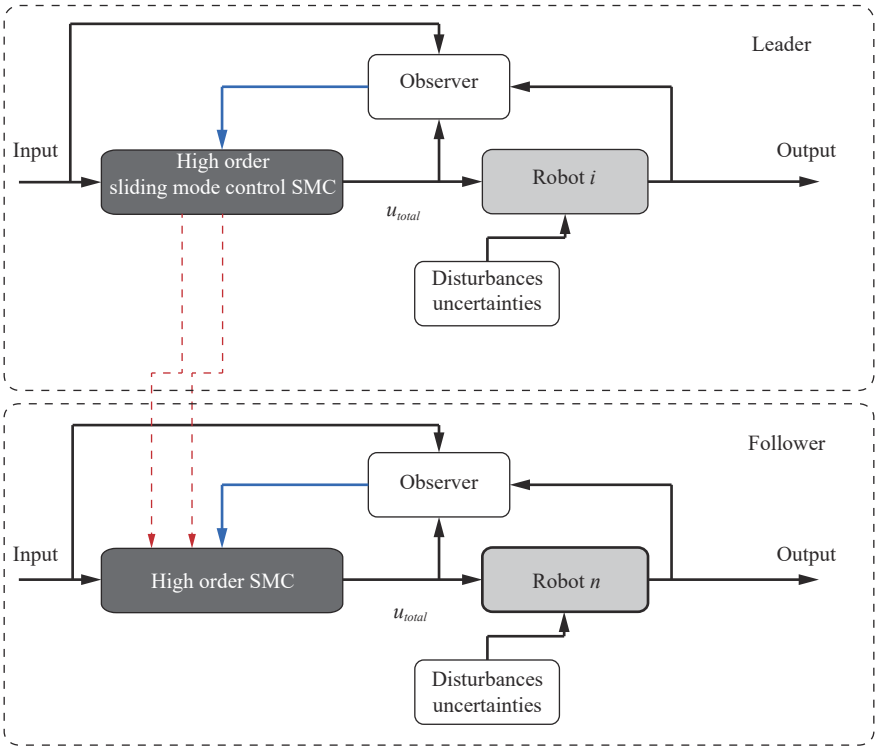

Fig. 3 Control scheme based on a leader-follower approach

then

$$L_\zeta = k_1|\zeta_1| + \frac{1}{2}\zeta_2^2. \tag{31}$$

The derivative of the previous equation is

$$\dot{L}_\zeta = \dot{\zeta}_1 k_1 \mathrm{sgn}(\zeta_1) + \zeta_2\dot{\zeta}_2. \tag{32}$$

By placing (28) and (29) into (32), (32) can be rewritten as

$$\dot{L}_\zeta = \zeta_2 k_1 \mathrm{sgn}(\zeta_1) - \zeta_2[k_1\mathrm{sgn}(\zeta_1) - k_2\mathrm{sgn}(\zeta_2)] \tag{33}$$

therefore,

$$\dot{L}_\zeta = -k_2|\zeta_2| \leq 0. \tag{34}$$

According to the Lassalle theorem, the derivative of Lyapunov function $\dot{L}_\zeta$ is zero, also $-k_2|\zeta_2|$ is obviously 0 and k_2 is positive definite. Then, ζ_2 is led to the origin (0) that means $\dot{\zeta}_1 = 0 \rightarrow \dot{\zeta}_2 = 0$, next $Z = \dot{Z} = 0$. Therefore, the overall system and observer are stable. With the integration of both sides of $\dot{L}_y = Z\dot{Z} \leq -\eta|Z|$ in order to get states, then

$$Z\frac{\mathrm{d}}{\mathrm{d}}tZ \leq -\eta|Z| \rightarrow \frac{Z}{|Z|}\mathrm{d}Z \leq -\eta\mathrm{d}t \rightarrow \int_{z_0}^{0}\frac{Z}{|Z|}\mathrm{d}Z \leq \int_0^{t_r} -\eta\mathrm{d}t. \tag{35}$$

These states have the absolute values, thus can be written as

$$\begin{aligned} f: Z>0 \rightarrow \int_{z_0}^{0} 1\mathrm{d}Z \leq \int_0^{t_r} -\eta\mathrm{d}t \rightarrow t_r \leq \frac{Z_0}{\eta} \\ f: Z>0 \rightarrow \int_{z_0}^{0} -1\mathrm{d}Z \leq \int_0^{t_r} -\eta\mathrm{d}t \rightarrow t_r \leq \frac{-Z_0}{\eta} \end{aligned} \tag{36}$$

in non-final states, the duration is not limited or when the sliding surface reaches 0, the duration is unknown.

$$t_r \leq \frac{|Z_0|}{\eta}. \tag{37}$$

The time parameter t can be set to reaching the sliding surface that it has been shown t_r. □

5 Checking the performance (simulation results)

In this section, a decentralized sliding mode cooperative control of two nonlinear multi-agent omini-directional robots is applied to demonstrate the power of the mentioned observer law. The windows-10 OS with Pentium-5 PC, Core 2 Duo 3.2-GHz CPU, 2 048-MB memory, and 1 024-MB VGA is used for simulation. And also the control scheme mentioned is implemented in Matlab, Simulink.

5.1 Example 1: MOWR with three wheels

Today, the need for MR is significantly growing[43,44]. According to the free movement of these robots, MRs can move with high flexibility and can do more duties than conventional robots[45–47]. The omnidirectional robot is the name for a special class of MRs where they can rotate around their centers of gravity and translation. Unlike conventional vehicles, the omnidirectional robots can control each of their degrees of freedom (DOFs) independently. They can move on complex trajectory paths and are able to maneuver in small spaces. Also, the probability of collision with objects is minimized according to the circular design of the robot. In Fig. 4, the motion system of the omnidirectional robot is displayed which is three wheels shifted 120 (degrees) and composed of passive rollers. This robot has three direct current (DC) motors with the gearbox in order to increase the torque. The DC motors are attached to the wheels which makes it able to achieve 3-DOF and the distance from the center of the robot to the center of each wheel is b. Equation (38) shows the state-space of the MOWR system that due to the Coulomb friction effect the model is nonlinear:

$$\frac{\mathrm{d}}{\mathrm{d}t}x_{i,n_i}(t) = f_i(x_{i,n_i}) + g_i u_i(t) + K_i\ \mathrm{sgn}(x_{i,n_i}) \tag{38}$$

where $[x_{i,1} = v,\ x_{i,2} = v_n,\ x_{i,3} = w]^{\mathrm{T}}$ is the state vector $x_{i,n_i}(t)$ such that the velocities mean the velocity of the robot frame. Fig. 5 displays the robot platform and three wheels with the DC motor as the driving force. $u(t) = [u_1, u_2, u_3]^{\mathrm{T}}$ shows the control input which is a continuous control signal. The angular velocity and linear velocity of the robot are v and v_n that are the orthogonal components of the omnidirectional robot platform and also the robot pose in the earth coordinate system is defined with vector w. Therefore, the states of the system are considered as follows:

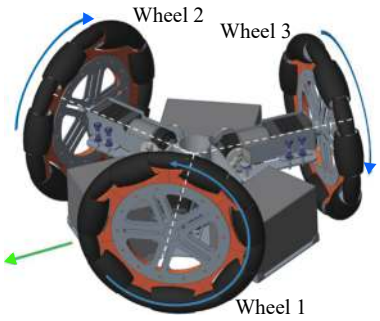

Fig. 4 Coordinate systems and geometric parameters

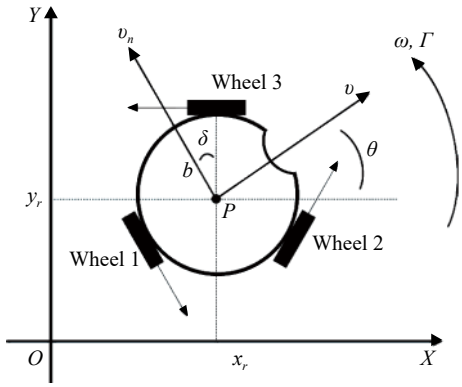

Fig. 5 Schematic of flexible-joint robot[48]

$$\begin{aligned}
\dot{x}_{i,1}[t] =& -\Gamma_1 x_{i,1}(t) + \Lambda_1 u_2(t) - \Lambda_1 u_3(t) - \\
& C_v M^{-1}\ \mathrm{sgn}[x_{i,1}(t)] \\
\dot{x}_{i,2}[t] =& -\Gamma_2 x_{i,2}(t) - \Lambda_2 u_1(t) + \Lambda_2 sen[\delta(u_2(t)) + u_3(t)] \\
& - C_{v_n} M^{-1}\ \mathrm{sgn}(x_{i,2}(t)) \\
\dot{x}_{i,3}[t] =& -\Gamma_3 x_{i,3}(t) - \Lambda_3[u_1(t) + u_2(t) + U_3(t)] - \\
& C_w M^{-1}\ \mathrm{sgn}(x_{i,3}(t))
\end{aligned} \tag{39}$$

and

$$\begin{aligned}
\Gamma_1 &= \frac{3l^2K_t^2 + 2R_a r^2 B_v}{2MR_a r^2} \\
\Gamma_2 &= \frac{3l^2K_t^2 + 2R_a r^2 B_{v_n}}{2MR_a r^2} \\
\Gamma_3 &= \frac{3l^2K_t^2 + 2MR_a r^2 B_w}{2MR_a r^2 I_n} \\
\Lambda_1 &= \frac{lK_t \cos(\delta_o)}{R_a r M} \\
\Lambda_2 &= \frac{lK_t}{R_a r M} \\
\Lambda_3 &= \frac{lK_t b}{R_a r I_n}
\end{aligned} \tag{40}$$

for the presented robot model, it is defined that $R_a = R_{a_{1,\cdots,3}}$, $K_t = K_{t_{1,\cdots,3}}$, $l = l_{1,\cdots,3}$ and $r = r_{1,\cdots,3}$. $L_{a_{1,\cdots,3}}$ parameters are ignored because they have little value. δ_o is represented $\frac{\pi}{6}$, b is the distance between the robot's center of mass and the wheels. B_v, B_{vn} and B_w are the viscous friction coefficients, the Coulomb friction coefficients are represented as C_v, C_{vn} and C_w. K_{ti}, L_{ai}, R_{ai}, r_i, l_i and i_{ai} are the torque constant, the armature inductance, resistance, wheels radius, motor reductions and armature currents, respectively. Consider the following dynamics of the robot for each agent as follows:

$$\begin{bmatrix} \dot{x}_{i,1}(t) \\ \dot{x}_{i,2}(t) \\ \dot{x}_{i,3}(t) \end{bmatrix} = A \begin{bmatrix} x_{i,1} \\ x_{i,2} \\ x_{i,3} \end{bmatrix} + B \begin{bmatrix} u_1 \\ u_2 \\ u_3 \end{bmatrix} + K\,\mathrm{sgn}\left(\begin{bmatrix} x_{i,1} \\ x_{i,2} \\ x_{i,3} \end{bmatrix} \right). \tag{41}$$

Table 1 depicts the geometric parameters, motor parameters, and the estimated parameters. Therefore, matrices A, B and K are given by

$$A = \begin{bmatrix} -3.63 & 0 & 0 \\ 0 & -3.51 & 0 \\ 0 & 0 & -5.69 \end{bmatrix}$$

$$B = \begin{bmatrix} -0.47 & 0 & 0.47 \\ 0.25 & -0.51 & 0.25 \\ 5.56 & 0.51 & 5.56 \end{bmatrix}$$

$$K = \begin{bmatrix} -0.98 & 0 & 0 \\ 0 & -1.05 & 0 \\ 0 & 0 & -6.06 \end{bmatrix}. \tag{42}$$

Fig. 6 reveals that all agents achieved consensus on the third state of the multi-agent system, and it is notable that the consensus has been reached in a short, limited time. In Fig. 7, the simulation results in the presence of measurement noise is displayed; all agents achieved consensus on the third state of the nonlinear MOWR. System responses under the high order sliding mode consensus protocol observer based controller for the proposed MOWR in the presence of measurement noise and the environmental disturbances are depicted in Fig. 8.

Table 1 Parameters of the ominidirectional robot (B is the viscous friction, C is Coulomb friction)

Parameter	Explanation	Value
B_v	For axis v	2
B_{v_n}	For axis v_n	1.5
B_w	For axis w	0.024
C_v	For axis v	1.2
C_{v_n}	For axis v_n	0.8
C_w	For axis w	0.003 5
b	Robot's radius	0.1 m
M	Robot's mass	1.5 kg
$L_{a_{1,\cdots,3}}$	Armature inductances	0.000 11
I_n	Robot's inertial momentum	0.025
$R_a = R_{a_{1,\cdots,3}}$	Armature resistances	1.66
δ	Angle	30°
$r = r_{1,\cdots,3}$	Wheels' radius	0.035
$l = l_{1,\cdots,3}$	Reduction	19:1
$K_t = K_{t_{1,\cdots,3}}$	Torque constants	0.005 9

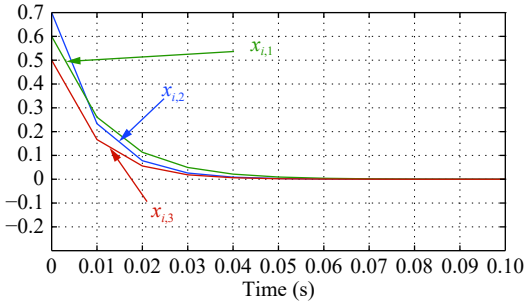

Fig. 6 State variables of three agents without noise

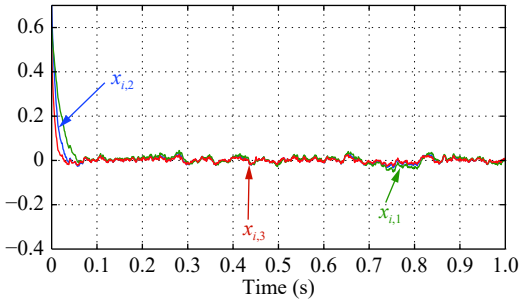

Fig. 7 State variables of three agents with noise $d(t)$

The simulation results demonstrated in this case are shown in Fig. 8. Fig. 8 depicts the state response of $x_{i,1}$, $x_{i,2}$ and $x_{i,3}$ for the closed-loop system.

A proportional integral derivative controller (PID) controller is presented to improve performance for control of the nonlinear multi-agent MOWR model and compare it with the proposed high order sliding mode consensus protocol observer-based controller. The PID controller is a generic control loop feedback mechanism and regarded as the standard control structure of the classical control theory. PID is the most commonly used feedback controller, literally everywhere in industrial applications. Minimizing the process error is the goal of the controller plan which continually adjusts the inputs. In this work, the parameters of the PID controller are obtained by trial and error method as $K_p = 2$, $K_i = 0.25$, and $K_d = 0.2$. Figs. 9 and 10 show the control inputs for the multi-agent omnidirectional wheeled robot system under the observer-based controller via the high order sliding mode consensus protocol and PID with noise and disturbance.

Figs. 11–13 reveal all agents achieved consensus on the third states of the multi-agent system, and it is notable that the consensus has been reached in a short, limited time. In Fig. 11, the simulation result is displayed for the multi-agent omnidirectional wheeled robot systems under an observer-based controller using the high order sliding mode consensus protocol and PID without noise that all agents achieved consensus on the third states of the nonlinear multi-agent omni-directional wheeled robot (ODWR). Fig. 12 shows response of the robot that this simulation is performed in the presence of the measurement noise. According to the responses, it can be said that all agents achieved consensus on the third states of the nonlinear multi-agent omni-directional wheeled robot. System responses under the high order sliding mode consensus protocol observer-based controller for the proposed MOWR in the presence of measurement noise and the environmental disturbance are depicted in Fig. 13. Figs. 11–13 depict the state response of the $x_{i,1}$, $x_{i,2}$ and $x_{i,3}$ for the closed-loop system.

5.2 Example 2: MOWR with four wheels

In order to investigate the performance of the proposed controller design, a MOWR system with four wheels is considered as Example 2. The MOWR is a good system to depict models with high nonlinearity equations, variation parameters and unmodeled dynamics. The wheel of MOWR includes a fixed standard wheel with passive rollers attached to the wheel circumference according to Fig. 14, where the angle between the wheel plane and the passive-roller rotation axis is 45 degrees.

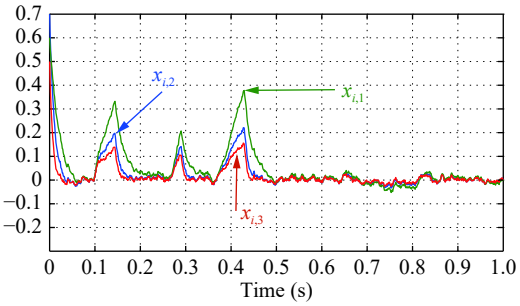

Fig. 8 State variables of three agents with noise and disturbance $d(t)$

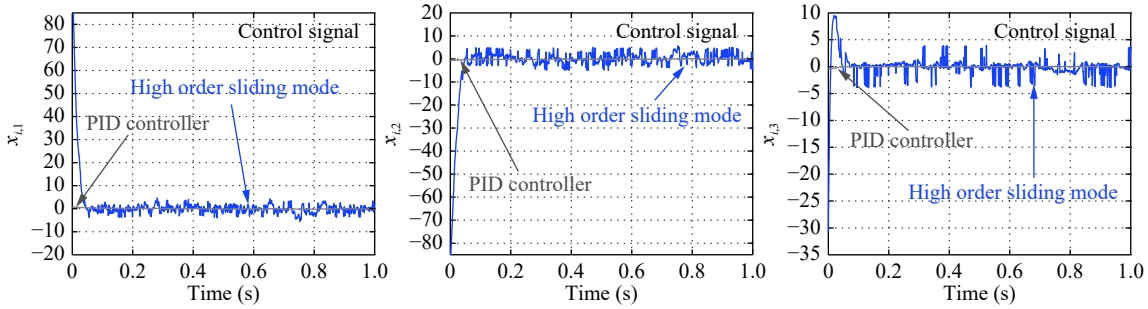

Fig. 9 Control inputs for the multi-agent omnidirectional wheeled robot system under observer-based controller using the high order sliding mode consensus protocol and PID with noise

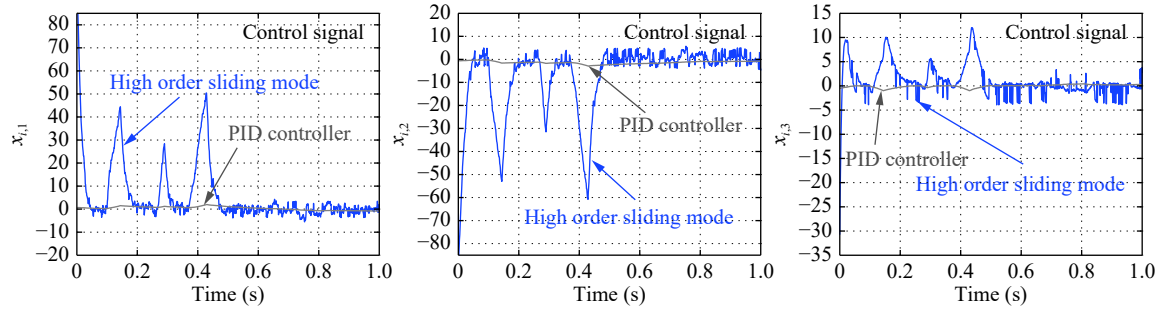

Fig. 10 Control inputs for the multi-agent omnidirectional wheeled robot system under observer-based controller using the high order sliding mode consensus protocol and PID with noise and disturbance

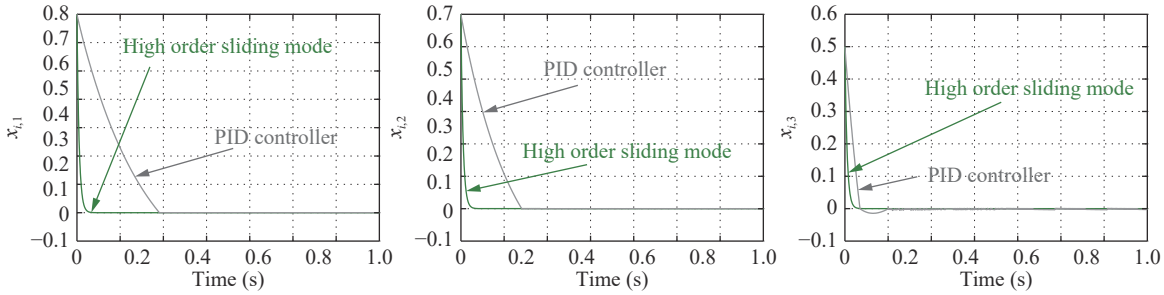

Fig. 11 State variable for the multi-agent omnidirectional wheeled robot systems under observer-based controller using the high order sliding mode consensus protocol and PID without noise

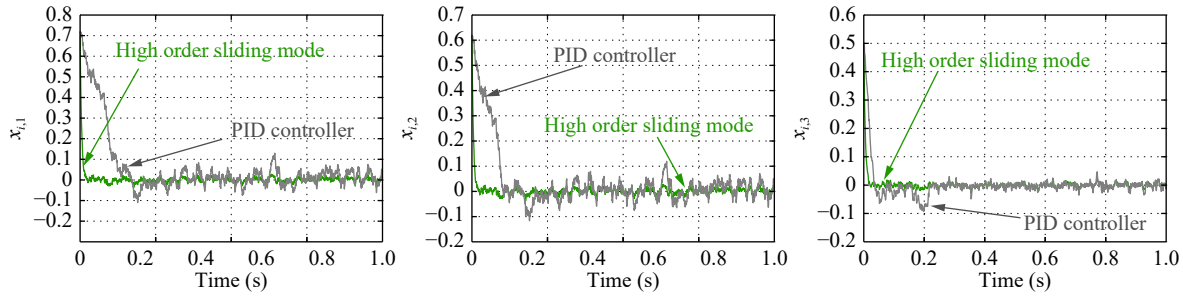

Fig. 12 State variable for the multi-agent omnidirectional wheeled robot systems under observer-based controller using the high order sliding mode consensus protocol and PID with noise

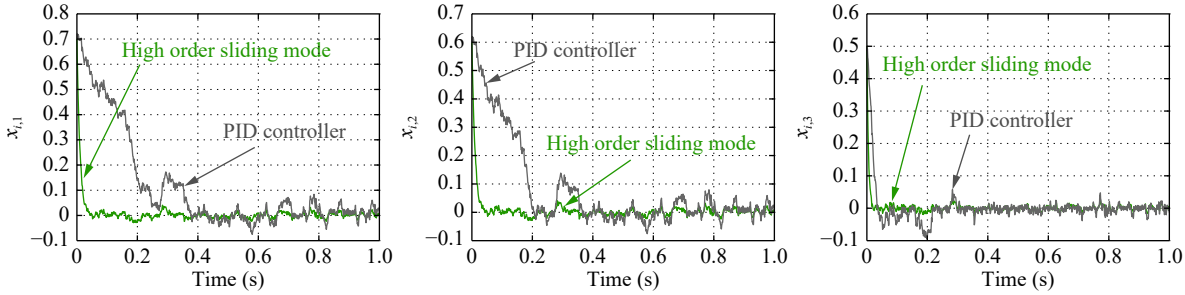

Fig. 13 State variable for the multi-agent omnidirectional wheeled robot systems under observer-based controller using the high order sliding mode consensus protocol and PID with noise and disturbance

Thus, the geometric parameters can be explained based on points A and G. A and G are the center point and the robot frame origin point, respectively. A wheel mounted on MOWR with local coordinate frame R, α is the angle of the vector GA from point G to point A, β is an angle that specifying the angle between the vector and the axis of the main wheel. So, the wheel center velocity component can be expressed as follows:

$$\begin{aligned}&\dot{x}_R \cos\left[\frac{\pi}{2} - \left(\frac{\pi}{2} - (\alpha+\beta)\right) - (\frac{\pi}{2} - \gamma)\right] + \\ &\dot{y}_R \cos\left[\frac{\pi}{2} - \left(\frac{\pi}{2} - (\alpha+\beta)\right) - (\frac{\pi}{2} - \gamma)\right] + \\ &l\dot{\theta} \cos\left[\alpha + \left(\frac{\pi}{2} - (\alpha+\beta)\right) - (\frac{\pi}{2} - \gamma)\right] \\ &= r\dot{\phi} \cos\gamma. \end{aligned} \tag{43}$$

l and γ are the distance from point G to point A and

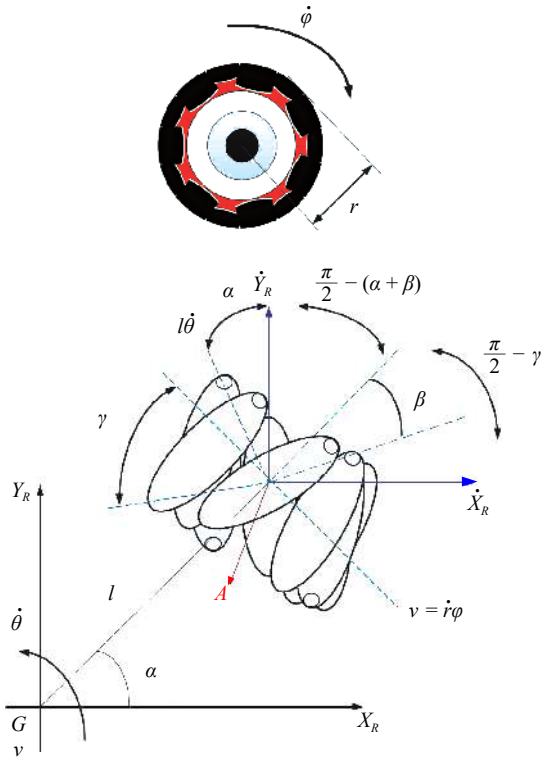

Fig. 14 Parameters of a Mecanum wheel

the main wheel's radius, respectively. $\dot{\phi}_{sw}$ is the passive roller that is in contact with the flat floor, $\dot{\phi}$ indicates the rotation speed of the main wheel. The junction between the two points of the floor and the Mecanum wheel is considered as an instantaneous rotation center. The mentioned velocity of point A is applied along the tangential direction because it is assumed to be in a pure rolling condition without slipping. Therefore, $r\dot{\phi}\cos(\gamma)$ is the velocity of the point A along the contact roller's axis. The rotation velocity about the Z axis and the translation velocity in terms of the local frame R are shown as the $\dot{x}_R$ and $\dot{y}_R$. Then,

$$\dot{x}_R\cos\Big[(\alpha+\beta+\gamma)-\frac{\pi}{2}\Big]+\dot{y}_R\cos[\pi-(\alpha+\beta+\gamma)]+ l\dot{\theta}\cos[\pi-(\beta+\gamma)]=r\dot{\phi}\cos\gamma. \tag{44}$$

Then, (44) is changed as follows:

$$\dot{x}_R\sin(\alpha+\beta+\gamma)-\dot{y}_R\cos(\alpha+\beta+\gamma)- l\dot{\theta}\cos(\beta+\gamma)=r\dot{\phi}\cos\gamma. \tag{45}$$

Therefore,

$$\begin{bmatrix}\sin(\alpha+\beta+\gamma)\\ -\cos(\alpha+\beta+\gamma)\\ \cos(\alpha+\beta+\gamma)\end{bmatrix}^{\mathrm{T}}\begin{bmatrix}\dot{x}_R\\ \dot{y}_R\\ \dot{\theta}\end{bmatrix}=r\dot{\phi}\cos\gamma. \tag{46}$$

The velocity can be received from the wheel's rotation speed because any kind of slip is not considered along the axis of the contact rollers in this model. Therefore, (46) is assumed as

$$\begin{bmatrix}\sin(\alpha+\beta+\gamma)\\ -\cos(\alpha+\beta+\gamma)\\ -l\cos(\beta+\gamma)\end{bmatrix}^{\mathrm{T}}\begin{bmatrix}\dot{x}_R\\ \dot{y}_R\\ \dot{\theta}\end{bmatrix}=r\dot{\phi}\cos\gamma. \tag{47}$$

R_i is the rotation matrix which represents the orientation of the inertia frame $\{I\}$ with respect to the robot frame $\{R\}$:

$$R_I(\theta)=\begin{bmatrix}\cos(\theta) & \sin(\theta) & 0\\ \sin(\theta) & \cos(\theta) & 0\\ 0 & 0 & 1\end{bmatrix}. \tag{48}$$

The angle between axes x_R and x_I is θ, the robot's velocity vector in terms of the robot frame, $\dot{\zeta}_R=[\dot{x}_R,\dot{y}_R,\dot{\theta}]^{\mathrm{T}}$ can be shown as $\dot{\zeta}_R=R_I(\theta)\dot{\zeta}_I$. The robot velocity vector in terms of the inertia frame I is ζ_I, (47) can be rewritten as follows:

$$\begin{bmatrix}\sin(\alpha+\beta+\gamma)\\ -\cos(\alpha+\beta+\gamma)\\ -l\cos(\beta+\gamma)\end{bmatrix}^{\mathrm{T}}R_I(\theta)\dot{\zeta}_I=r\dot{\phi}\cos\gamma. \tag{49}$$

According to the free rotation of the passive contact roller, the motion is not constrained. Therefore, the velocity relation is given as follows:

$$\begin{aligned}&\dot{x}_R\sin\Big[\frac{\pi}{2}-\Big(\frac{\pi}{2}-(\alpha+\beta)\Big)-(\frac{\pi}{2}-\gamma)\Big]-\\ &\quad\dot{y}_R\sin\Big[\Big(\frac{\pi}{2}-(\alpha+\beta)\Big)+(\frac{\pi}{2}-\gamma)\Big]+\\ &\quad l\dot{\theta}\sin\Big[\alpha+\Big(\frac{\pi}{2}-(\alpha+\beta)\Big)+(\frac{\pi}{2}-\gamma).\Big]\\ &=-r\dot{\phi}\cos\gamma-r_{sw}\dot{\phi}_{sw}\end{aligned} \tag{50}$$

and

$$\begin{bmatrix}\cos(\alpha+\beta+\gamma)\\ \sin(\alpha+\beta+\gamma)\\ l\cos(\beta+\gamma)\end{bmatrix}^{\mathrm{T}}\begin{bmatrix}\dot{x}_R\\ \dot{y}_R\\ \dot{\theta}\end{bmatrix}+r\dot{\phi}\sin\gamma+r_{sw}\dot{\phi}_{sw}=0. \tag{51}$$

So, (50) can be transformed as

$$\begin{bmatrix}\cos(\alpha+\beta+\gamma)\\ \sin(\alpha+\beta+\gamma)\\ l\cos(\beta+\gamma)\end{bmatrix}^{\mathrm{T}}R_I(\theta)\dot{\zeta}_I+r\dot{\phi}\sin\gamma+r_{sw}\dot{\phi}_{sw}=0. \tag{52}$$

Table 2 presents the angles α_i, β_i and γ of the four Mecanum wheels. Fig. 15 depicts the omnidirectional wheeled robot (OWR) platform with four Mecanum

Table 2 Parameters of the Mecanum wheels

Wheels	α_i	β_i	γ_i
1	$\tan^{-1}\left(\frac{b}{a}\right)$	$-\tan^{-1}\left(\frac{b}{a}\right)$	$\left(\frac{\pi}{2}+\frac{\pi}{4}\right)$
2	$\pi-\tan^{-1}\left(\frac{b}{a}\right)$	$\tan^{-1}\left(\frac{b}{a}\right)$	$-\left(\frac{\pi}{2}+\frac{\pi}{4}\right)$
3	$\pi+\tan^{-1}\left(\frac{b}{a}\right)$	$-\tan^{-1}\left(\frac{b}{a}\right)$	$\left(\frac{\pi}{2}+\frac{\pi}{4}\right)$
4	$2\pi-\tan^{-1}\left(\frac{b}{a}\right)$	$\tan^{-1}\left(\frac{b}{a}\right)$	$-\left(\frac{\pi}{2}+\frac{\pi}{4}\right)$

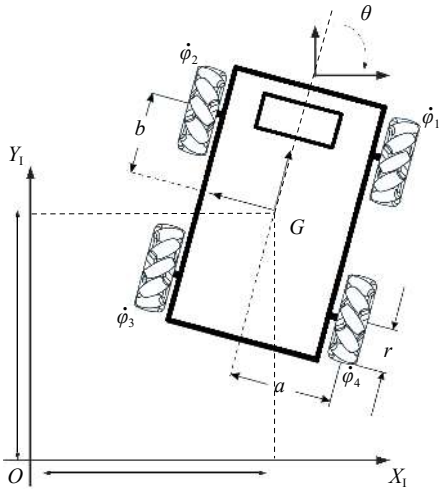

Fig. 15 A multi-agent omnidirectional wheeled robot

wheels. The dynamic equations for the four-wheel centers are given as follows:

$$\begin{bmatrix} \sin(\alpha_1+\beta_1+\gamma_1) & \cos(\alpha_1+\beta_1+\gamma_1) & -l_1\cos(\beta_1+\gamma_1) \\ \sin(\alpha_2+\beta_2+\gamma_2) & \cos(\alpha_2+\beta_2+\gamma_2) & -l_2\cos(\beta_2+\gamma_2) \\ \sin(\alpha_3+\beta_3+\gamma_3) & \cos(\alpha_3+\beta_3+\gamma_3) & -l_3\cos(\beta_3+\gamma_3) \\ \sin(\alpha_4+\beta_4+\gamma_4) & \cos(\alpha_4+\beta_4+\gamma_4) & -l_4\cos(\beta_4+\gamma_4) \end{bmatrix} \times$$

$$R_I(\theta)\dot{\zeta}_I = \begin{bmatrix} r_1\dot{\phi}_1\cos\gamma_1 \\ r_2\dot{\phi}_2\cos\gamma_2 \\ r_3\dot{\phi}_3\cos\gamma_3 \\ r_4\dot{\phi}_4\cos\gamma_4 \end{bmatrix}. \tag{53}$$

This part assumes that each wheel has an equal radius and distance. Hence, the inverse kinematics equation is defined as follows:

$$\begin{bmatrix} \dot{\phi}_1 \\ \dot{\phi}_2 \\ \dot{\phi}_3 \\ \dot{\phi}_4 \end{bmatrix} = -\frac{\sqrt{(2)}}{r} J \begin{bmatrix} \dot{x}_R \\ \dot{y}_R \\ \dot{\theta} \end{bmatrix} \tag{54}$$

where $\alpha = \tan^{-1}\left(\frac{b}{a}\right)$, and J is the Jacobian matrix:

$$J = \begin{bmatrix} \left(\frac{\sqrt{(2)}}{2}\right), & \left(\frac{\sqrt{(2)}}{2}\right), & l\sin\left(\frac{\pi}{4}-\alpha\right) \\ \left(\frac{\sqrt{(2)}}{2}\right), & -\left(\frac{\sqrt{(2)}}{2}\right), & l\sin\left(\frac{\pi}{4}-\alpha\right) \\ -\left(\frac{\sqrt{(2)}}{2}\right), & -\left(\frac{\sqrt{(2)}}{2}\right), & l\sin\left(\frac{\pi}{4}-\alpha\right) \\ -\left(\frac{\sqrt{(2)}}{2}\right), & \left(\frac{\sqrt{(2)}}{2}\right), & l\sin\left(\frac{\pi}{4}-\alpha\right) \end{bmatrix} \times$$

$$\begin{bmatrix} \cos\theta & \sin\theta & 0 \\ \sin\theta & \cos\theta & 0 \\ 0 & 0 & 1 \end{bmatrix}. \tag{55}$$

Equation (55) shows the forward kinematics equation of the multi-agent omnidirectional wheeled robot system:

$$q_i = [\dot{x}_{i,1}, \dot{x}_{i,2}, \dot{x}_{i,3}]^{\mathrm{T}} = -\frac{\sqrt{(2)}}{2} r J_i \begin{bmatrix} u_1 \\ u_2 \\ u_3 \\ u_4 \end{bmatrix} \tag{56}$$

where the states of the robot are $x_{i,1} = x_R$, $x_{i,2} = y_R$ and $x_{i,3} = \theta$. The pseudoinverse of J is $J_i = (J^{\mathrm{T}}J)^{-1}J^{\mathrm{T}}$, the control input u is $[\dot{\phi}_1, \dot{\phi}_2, \dot{\phi}_3, \dot{\phi}_4]^{\mathrm{T}}$. In the simulation, a leader agent and three follower agents are considered, the general purpose of the consensus protocol is that the consensus moves within a limited time. Initial conditions to simulate a multi-factor controller are considered as $q_1(0) = [2, 2, 2]^{\mathrm{T}}$, $q_2(0) = [1, 1, 1]^{\mathrm{T}}$, $q_3(0) = -[1, 1, 1]^{\mathrm{T}}$ and $q_4(0) = [-2, -2, -2]^{\mathrm{T}}$, and also their initial velocities are zero. Fig. 16 reveals that all agents achieved consensus on the third state of the multi-agent system, and it is notable that the consensus has been reached in a short, limited time. In Fig. 16, the simulation result is displayed for the multi-agent omnidirectional wheeled robot systems under an observer-based controller using the high order sliding mode consensus protocol without noise; all agents achieved consensus on the third state of the nonlinear MOWR. Fig. 17 shows the simulation result in the presence of measurement noise, in which all agents achieved consensus on the third state of the nonlinear MOWR.

System responses under the sliding mode observer-based controller with consensus protocol for the proposed robot in the presence of measurement noise and the environmental disturbance are depicted in Fig. 18. Figs. 16–18 depict the state response of the $x_{i,1}$, $x_{i,2}$ and $x_{i,3}$ for the closed-loop system.

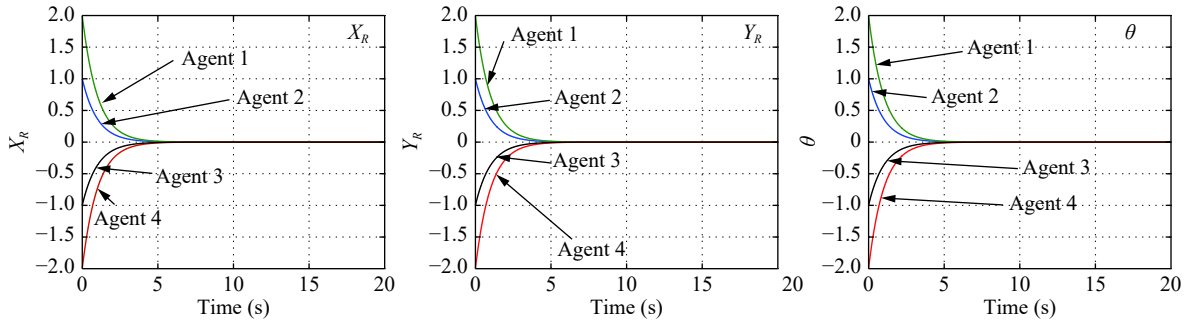

Fig. 16 Third variable state of four agents without noise under the high order sliding mode consensus protocol

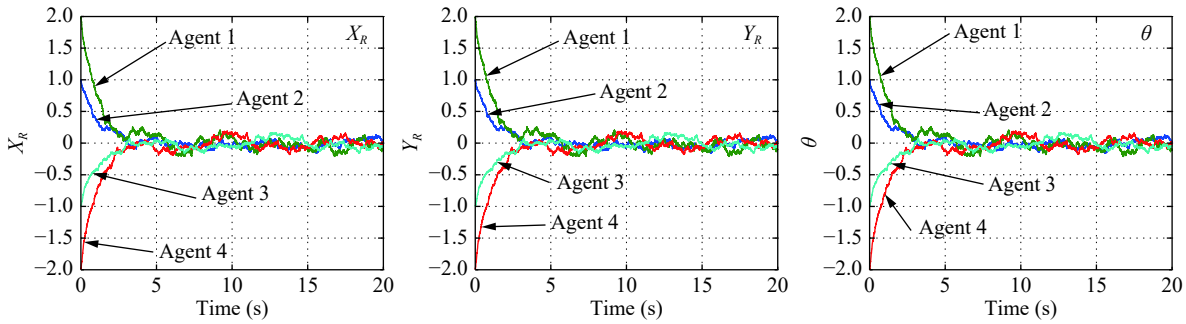

Fig. 17 Third variable state of four agents with noise under the high order sliding mode consensus protocol

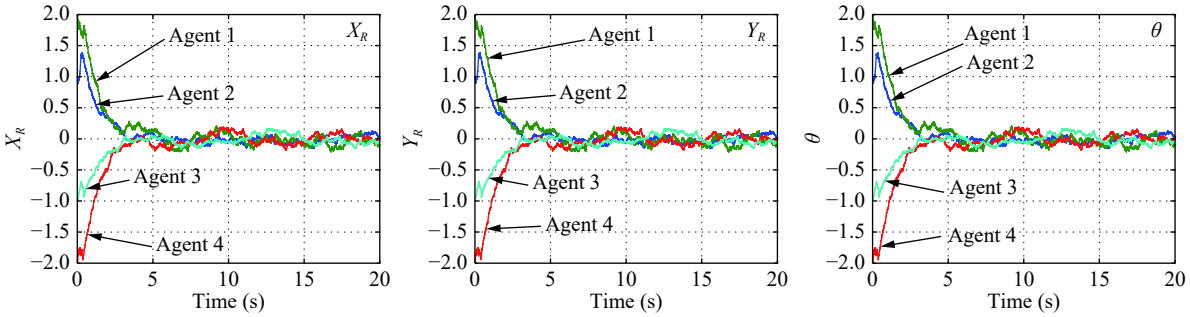

Fig. 18 Third variable state of four agents with noise and disturbance under the high order sliding mode consensus protocol

6 Conclusions

A novel observer-based control of the nonlinear multi-agent robot models using the high order sliding mode consensus protocol was proposed in this paper. The promising performance in the closed-loop system was shown via the combination of the robust sliding mode observer and the adaptive controller. Theoretical analysis by a candidate Lyapunov function had been presented to show the stability of the overall MAS, the convergence of observer and tracking error to zero, and the reduction of the chattering phenomena. Furthermore, the proposed method ensures all signals involved in MAS were uniformly ultimately bounded and the system was robust against the external disturbances and uncertainties. The observer was applied to a nonlinear multi-agent omnidirectional wheeled robot in order to illustrate the promising performance of the methodology. To illustrate the promising performance of the methodology, the observer was used on a nonlinear multi-agent omnidirectional wheeled robot. The results displayed the meritorious performance of the scheme.

References

[1] M. R. R. Khoygani, R. Ghasemi, A. R. Vali. Intelligent nonlinear observer design for a class of nonlinear discrete-time flexible joint robot. *Intelligent Service Robotics*, vol. 8, no. 1, pp. 45–56, 2015. DOI: 10.1007/s11370-014-0162-x.

[2] S. R. Sahoo, S. S. Chiddarwar. Flatness-based control scheme for hardware-in-the-loop simulations of omnidirectional mobile robot. *Simulation*, vol. 96, no. 2, pp. 169–183, 2020. DOI: 10.1177/0037549719859064.

[3] V. Alakshendra, S. S. Chiddarwar. Adaptive robust control of Mecanum-wheeled mobile robot with uncertainties. *Nonlinear Dynamics*, vol. 87, no. 4, pp. 2147–2169, 2017. DOI: 10.1007/s11071-016-3179-1.

[4] V. Alakshendra, S. S. Chiddarwar. Simultaneous balancing and trajectory tracking control for an omnidirectional mobile robot with a cylinder using switching between two robust controllers. *International Journal of Advanced Robotic Systems*, vol. 14, no. 6, pp. 1–16, 2017. DOI: 10.1177/1729881417738728.

[5] B. E. Byambasuren, D. Kim, M. Oyun-Erdene, C. Bold, J. Yura. Inspection robot based mobile sensing and power line tracking for smart grid. *Sensors*, vol. 16, no. 2, Article number 250, 2016. DOI: 10.3390/s16020250.

[6] J. M. Bengochea-Guevara, J. Conesa-Munoz, D. Andujar, A. Ribeiro. Merge fuzzy visual servoing and GPS-based planning to obtain a proper navigation behavior for a small crop-inspection robot. *Sensors*, vol. 16, no. 3, Article number 276, 2016. DOI: 10.3390/s16030276.

[7] J. G. Blitch. Artificial intelligence technologies for robot assisted urban search and rescue. *Expert Systems with Applications*, vol. 11, no. 2, pp. 109–124, 1996. DOI: 10.1016/0957-4174(96)00038-3.

[8] S. Fish. UGVs in future combat systems. In *Proceedings of SPIE 5422, Unmanned Ground Vehicle Technology VI, Defense and Security*, SPIE, Orlando, USA, pp. 288–291, 2004. DOI: 10.1117/12.537966.

[9] J. Lafaye, D. Gouaillier, P. B. Wieber. Linear model predictive control of the locomotion of Pepper, a humanoid robot with omnidirectional wheels. In *Proceedings of IEEE-RAS International Conference on Humanoid Robots*, IEEE, Madrid, Spain, pp. 336–341, 2014. DOI: 10.1109/HUMANOIDS.2014.7041381.

[10] M. Wada, H. H. Asada. Design and control of a variable footprint mechanism for holonomic omnidirectional vehicles and its application to wheelchairs. *IEEE Transactions on Robotics and Automation*, vol. 15, no. 6, pp. 978–989, 1999. DOI: 10.1109/70.817663.

[11] United Nations. World Population Ageing 2013, [Online], Available: https://www.un.org/en/development/desa/population/publications/pdf/ageing/WorldPopulationAgeing2013.pdf, December 15, 2015.

[12] World Health Organization. World Report on Ageing and Health, [Online], Available: http://apps.who.int/iris/bitstream/10665/186463/1/9789240694811-eng.pdf, February 18, 2016.

[13] C. Moron, A. Payan, A. Garcia, F. Bosquet. Domotics project housing block. *Sensors*, vol. 16, no. 5, Article number 741, 2016. DOI: 10.3390/s16050741.

[14] E. Clotet, D. Martinez, J. Moreno, M. Tresanchez, J. Palacin. Assistant Personal Robot (APR): Conception and application of a Tele-operated assisted living robot. *Sensors*, vol. 16, no. 5, Article number 610, 2016. DOI: 10.3390/s16050610.

[15] M. Tavakoli, J. Lourenco, C. Viegas, P. Neto, A. T. De Almeida. The hybrid OmniClimber robot: Wheel based climbing, arm based plane transition, and switchable magnet adhesion. *Mechatronics*, vol. 36, pp. 136–146, 2016. DOI: 10.1016/j.mechatronics.2016.03.007.

[16] J. Santos, A. Conceicao, T. Santos, H. Araujo. Remote control of an omnidirectional mobile robot with time-varying delay and noise attenuation. *Mechatronics*, vol. 52, pp. 7–21, 2018. DOI: 10.1016/j.mechatronics.2018.04.003.

[17] D. B. Zhao, J. Q. Yi. *Introduction to Omni-directional Mobile Robot*, Beijing, China: Science Press, 2010. (in Chinese)

[18] X. Y. Deng, J. Q. Yi, D. B. Zhao. Kinematic analysis of an omni-directional mobile robot. *Robot*, vol. 26, no. 1, pp. 49–53, 2004. DOI: 10.3321/j.issn:1002-0446.2004.01.011. (in Chinese)

[19] C. Ren, S. G. Ma. Trajectory tracking control of an omnidirectional mobile robot with friction compensation. In *Proceedings of IEEE/RSJ International Conference on Intelligent Robots and Systems*, IEEE, Daejeon, South Korea, pp. 5361–5366, 2016. DOI: 10.1109/IROS.2016.7759788.

[20] H. P. Oliveira, A. J. Sousa, A. P. Moreira, P. J. Costa. Dynamical models for omni-directional robots with 3 and 4 wheels. In *Proceedings of the 5th International Conference on Informatics in Control, Automation and Robotics*, INSTICC Press, Madeira, Portugal, pp. 189–196, 2008.

[21] C. Sprunk, B. Lau, P. Pfaff, W. Burgard. An accurate and efficient navigation system for omnidirectional robots in industrial environments. *Autonomous Robots*, vol. 41, no. 2, pp. 473–493, 2017. DOI: 10.1007/s10514-016-9557-1.

[22] D. S. Lal, A. Vivek. Dynamic modeling and control of omni-directional mobile robots. In *Proceedings of IEEE International Conference on Circuit, Power and Computing Technologies*, IEEE, Kollam, India, pp. 1–7, 2017. DOI: 10.1109/ICCPCT.2017.8074219.

[23] T. F. Wu, H. C. Huang, P. S. Tsai, N. T. Hu, Z. Q. Yang. The tracking control design of adaptive fuzzy CMAC for an omni-directional mobile robot. *Journal of Computers*, vol. 28, no. 1, pp. 247–260, 2017. DOI: 10.3966/199115592017022801019.

[24] D. Xu, D. B. Zhao, J. Q. Yi, X. M. Tan. Trajectory tracking control of omnidirectional wheeled mobile manipulators: Robust neural network-based sliding mode approach. *IEEE Transactions on Systems, Man, and Cybernetics Part B: Cybernetics*, vol. 39, no. 3, pp. 788–799, 2009. DOI: 10.1109/TSMCB.2008.2009464.

[25] C. C. Tsai, H. L.Wu, F. C. Tai, Y. S. Chen. Distributed consensus formation control with collision and obstacle avoidance for uncertain networked omnidirectional multi-robot systems using fuzzy wavelet neural networks. *International Journal of Fuzzy Systems*, vol. 19, no. 5, pp. 1375–1391, 2017. DOI: 10.1007/s40815-016-0239-0.

[26] M. Fatima, H. Assia, H. Habib. Adaptive nonlinear control of a synchronous generator. *Carpathian Journal of Electronic and Computer Engineering*, vol. 11, no. 2, pp. 39–43, 2018. DOI: 10.2478/cjece-2018-0017.

[27] M. P. Aghababa. Robust stabilization and synchronization of a class of fractional-order chaotic systems via a novel fractional sliding mode controller. *Communications in Nonlinear Science and Numerical Simulation*, vol. 17, no. 6, pp. 2670–2681, 2012. DOI: 10.1016/j.cnsns.2011.10.028.

[28] K. Shojaei, A. M. Shahri. Adaptive robust time-varying control of uncertain non-holonomic robotic systems. *IET Control Theory & Applications*, vol. 6, no. 1, pp. 90–102, 2012. DOI: 10.1049/iet-cta.2010.0655.

[29] S. T. Kao, W. J. Chiou, M. T. Ho. Integral sliding mode control for trajectory tracking control of an omnidirectional mobile robot. In *Proceedings of the 8th Asian Control Conference*, IEEE, Kaohsiung, China, pp. 765–770, 2011.

[30] S. V. Drakunov, V. I. Utkin. Sliding mode control in dynamic systems. *International Journal of Control*, vol. 55, no. 4, pp. 1029–1037, 1992. DOI: 10.1080/00207179208934270.

[31] L. Long, D. B. Ren, J. Y. Zhang. Terminal sliding mode control for vehicle longitudinal following in automated highway system. In *Proceedings of the 27th Chinese Control Conference*, IEEE, Kunming, China, pp. 605–608, 2008. DOI: 10.1109/CHICC.2008.4605782.

[32] Y. H. Chang, C. W. Chang, W. C. Chan. Fuzzy sliding-mode consensus control for multi-agent systems. In *Proceedings of American Control Conference*, IEEE, San Francisco, USA, pp. 1636–1641, 2011. DOI: 10.1109/ACC.

2011.5991103.

[33] C. W. Chang, C. L. Chen, Y. H. Chang, C. W. Tao. Adaptive fuzzy sliding-mode formation control for second-order multi-agent systems. In *Proceedings of International Conference on System Science and Engineering*, IEEE, Taipei, China, pp. 310–314, 2010. DOI: 10.1109/ICSSE.2010.5551778.

[34] S. Muhammad, M. Idrees. Comparative study of hierarchical sliding mode control and decoupled sliding mode control. In *Proceedings of the 12th IEEE Conference on Industrial Electronics and Applications*, IEEE, Siem Reap, Cambodia, pp. 818–824, 2017. DOI: 10.1109/ICIEA.2017.8282952.

[35] S. Alvarez-Rodriguez, G. Flores, N. A. Ochoa. Variable gains sliding mode control. *International Journal of Control, Automation and Systems*, vol. 17, no. 3, pp. 555–564, 2019. DOI: 10.1007/s12555-018-0095-9.

[36] N. Zhao, J. D. Zhu. Sliding mode control for robust consensus of linear multi-agent systems. In *Proceedings of the 10th World Congress on Intelligent Control and Automation*, IEEE, Beijing, China, pp. 1378–1382, 2012. DOI: 10.1109/WCICA.2012.6358095.

[37] M. R. James, J. S. Baras. An observer design for nonlinear control systems. *Analysis and Optimization of Systems*, A. Bensoussan, J. L. Lions, Eds., Berlin Heidelberg, Germany: Springer, pp. 170–180, 1988. DOI: 10.1007/BFb0042212.

[38] V. Gazi, B. Fidan. Coordination and control of multi-agent dynamic systems: Models and approaches. *Swarm Robotics*, E. Sahin, W. M. Spears, A. F. T. Winfield, Eds., Berlin Heidelberg, Germany: Springer, pp. 71–102, 2007. DOI: 10.1007/978-3-540-71541-2_6.

[39] X. J. Long, S. H. Yu, Y. L. Wang, L. N. Jin. Leader-follower consensus of multi-agent system with external disturbance based on integral sliding mode control. In *Proceedings of the 33rd Chinese Control Conference*, IEEE, Nanjing, China, pp. 1740–1745, 2014. DOI: 10.1109/ChiCC.2014.6896891.

[40] U. B. Kamble, J. O. Chandle, V. S. Lahire, R. D. Langde. Second order twisting sliding mode control of multi-agent network with input disturbance. In *Proceedings of Fourth International Conference on Computing, Communications and Networking Technologies*, IEEE, Tiruchengode, India, 2013. DOI: 10.1109/ICCCNT.2013.6726495.

[41] C. E. Ren, C. L. P. Chen. Sliding mode leader-following consensus controllers for second-order non-linear multi-agent systems. *IET Control Theory & Applications*, vol. 9, no. 10, pp. 1544–1552, 2015. DOI: 10.1049/iet-cta.2014.0523.

[42] H. K. Khalil. *Nonlinear Systems*, 3rd ed., New York, USA: Prentice-Hall, 2001.

[43] M. Panda, B. Das, B. Subudhi, B. B. Pati. A comprehensive review of path planning algorithms for autonomous underwater vehicles. *International Journal of Automation and Computing*, vol. 17, no. 3, pp. 321–352, 2020. DOI: 10.1007/s11633-019-1204-9.

[44] N. Hacene, B. Mendil. Fuzzy behavior-based control of three wheeled omnidirectional mobile robot. *International Journal of Automation and Computing*, vol. 16, no. 2, pp. 163–185, 2019. DOI: 10.1007/s11633-018-1135-x.

[45] A. Kumar, A. Ojha. Experimental evaluation of certain pursuit and evasion schemes for wheeled mobile robots. *International Journal of Automation and Computing*, vol. 16, no. 4, pp. 491–510, 2019. DOI: 10.1007/s11633-018-1151-x.

[46] I. Ardiyanto, J. Miura. Time-space viewpoint planning for guard robot with chance constraint. *International Journal of Automation and Computing*, vol. 16, no. 4, pp. 475–490, 2019. DOI: 10.1007/s11633-018-1146-7.

[47] H. X. Ma, W. Zou, Z. Zhu, C. Zhang, Z. B. Kang. Selection of observation position and orientation in visual servoing with eye-in-vehicle configuration for manipulator. *International Journal of Automation and Computing*, vol. 16, no. 6, pp. 761–774, 2019. DOI: 10.1007/s11633-019-1181-z.

[48] J. Moreno, E. Clotet, R. Lupianez, M. Tresanchez, D. Martinez, T. Palleja, J. Casanovas, J. Palacin. Design, implementation and validation of the three-wheel holonomic motion system of the assistant personal robot (APR). *Sensors*, vol. 16, no. 10, Article number 1658, 2016. DOI: 10.3390/s16101658.

M. R. Rahimi Khoygani received the B. Sc. degree in electrical power engineering from the Islamic Azad University (IAU), Iran in 2012, the M. Sc. degree in control engineering from IAU, Iran in 2015. He is currently a member of Department of Control Engineering, Qom University, Iran.

His research interests include neural net, fuzzy systems, intelligent systems, robotics, control of nonlinear systems, nonlinear observer, intelligent state estimation, and adaptive control.

E-mail: mrrahimikh@gmail.com (Corresponding author)
ORCID iD: 0000-0002-0231-7701

R. Ghasemi received the B. Sc. degree in electrical engineering from Semnan University, Iran in 2000, and the M. Sc. and Ph. D. degrees in control engineering from Amirkabir University of Technology, Iran in 2004 and 2009, respectively. He joined Department of Electrical Engineering, Qom University, Iran, where he is currently a professor of electrical engineering.

His research interests include large-scale systems, adaptive control, robust control, nonlinear control, and intelligent systems.

E-mail: r.ghasemi@qom.ac.ir

P. Ghayoomi received the B. Sc. and M. Sc. degrees in control engineering from Islamic Azad University, Iran in 2013 and 2016, respectively. He is currently a member of Department of Control Engineering, Qom University, Iran.

His research interests include intelligent systems, robotics, nonlinear observer, and adaptive control.

E-mail: pooriyaghayoomi@gmail.com

International Journal of Automation & Computing

Citation: M. R. Rahimi Khoygani, R. Ghasemi, P. Ghayoomi. Robust observer–based control of nonlinear multi–omnidirectional wheeled robot systems via high order sliding–mode consensus protocol. *International Journal of Automation and Computing*, vol.18, no.5, pp.787–801, 2021. https://doi.org/10.1007/s11633–020–1254–z